Clin Exp Metastasis (2009) 26:599–610
DOI 10.1007/s10585-009-9259-6

RESEARCH PAPER

# Establishment and characterization of a new highly metastatic human osteosarcoma cell line

**Yuxi Su · Xiaoji Luo · Bai-Cheng He · Yi Wang · Liang Chen · Guo-Wei Zuo · Bo Liu · Yang Bi · Jiayi Huang · Gao-Hui Zhu · Yun He · Quan Kang · Jinyong Luo · Jikun Shen · Jin Chen · Xianqing Jin · Rex C. Haydon · Tong-Chuan He · Hue H. Luu**

Received: 13 January 2009 / Accepted: 4 March 2009 / Published online: 11 April 2009


**Abstract** Osteosarcoma is the most common primary malignancy of bone in children and young adults. There is a paucity of tumorigenic and highly metastatic human osteosarcoma cell lines that have not been further transformed by exogenous means. Here we establish and characterize a highly metastatic human osteosarcoma cell line that is derived from a poorly metastatic MG63 line through serial passage in nude mice via intratibial injections. The occasional pulmonary metastases developed from MG63 were harvested and repassaged in mice until a highly metastatic subline (MG63.2) was established. The parental MG63 and highly metastatic MG63.2 cells were further characterized in vitro and in vivo. MG63.2 cells demonstrated increased cell migration and invasion compared to the parental MG63 cells. Conversely, cell adhesion was significantly greater in MG63 cells when compared to the MG63.2 cells. MG63.2 cells grew at a slightly slower rate than that of the parental cells. When injected into nude mice, MG63.2 cells had a greater than 200-fold increase in developing pulmonary metastases compared to the parental MG63 cells. MG63.2 cells also formed larger primary tumors when compared to the parental MG63 cells. Further analysis revealed that ezrin expression was up-regulated in the metastatic MG63.2 cells. Interestingly, expressions of MMP-2 and MMP-9 were down-regulated, and expression of TIMP-2 was up-regulated in the MG63.2 cells. Taken together, we have established and characterized a highly metastatic human osteosarcoma cell line that should serve as a valuable tool for future investigations on the pathogenesis, metastasis, and potential treatments of human osteosarcoma.

**Keywords** Animal model · Ezrin · Osteosarcoma · Matrix metalloproteinase · Metastasis

Y. Su · X. Luo · B.-C. He · Y. Wang · L. Chen · G.-W. Zuo · B. Liu · Y. Bi · J. Huang · G.-H. Zhu · Y. He · Q. Kang · J. Luo · J. Chen · X. Jin · T.-C. He
The Children's Hospital and Key Laboratory of Diagnostic Medicine Designated by the Ministry of Education of China, Chongqing Medical University, 400016 Chongqing, China

Y. Su · X. Luo · B.-C. He · Y. Wang · L. Chen · G.-W. Zuo · B. Liu · Y. Bi · J. Huang · G.-H. Zhu · Y. He · Q. Kang · J. Luo · J. Shen · J. Chen · R. C. Haydon · T.-C. He · H. H. Luu (✉)
Molecular Oncology Laboratory, Department of Surgery, The University of Chicago Medical Center, 5841 South Maryland Avenue, MC3079, Chicago, IL 60637, USA
e-mail: hluu@surgery.bsd.uchicago.edu

## Introduction

Osteosarcoma is the most common primary malignancy of bone and primarily affects young individuals [1, 2]. Over 80% of osteosarcoma patients have metastatic or micrometastatic disease at the time they are diagnosed [3–6]. In the vast majority of patients, the site of metastasis is usually the lungs [7–9]. As a result of the common occurrence of metastases, nearly all patients receive neo-adjuvant and adjuvant chemotherapy to treat the presumed disseminated systemic disease while surgery is used to treat local disease [10]. Prior to the advent of chemotherapy, surgery involved amputations and the survival in osteosarcoma patients was ~20%, which was a reflection of the 20% of patients who never developed metastases. Current treatment for osteosarcoma patients includes chemotherapy and surgery,

which often involves limb salvage surgery. Survival now approaches 65–75% with the current regimen [10–12]. Although we have made advances in improving survival compared to three decades ago, there seems to be a plateau in the improved survival of our patients [10]. This may reflect the fact that our understanding of molecular and cellular events leading to the development and metastasis of osteosarcoma remains limited [13]. In fact, the genetic event(s) leading to the development of human osteosarcoma are not known [13]. While Rb and p53 mutations have been identified in a subset of osteosarcoma patients, there are as of yet no unifying genetic alterations in osteosarcoma [14–18].

On the other hand, clinically relevant animal models are critical to the understanding of the basic mechanism of osteosarcoma development and metastasis, as well as for the development of novel therapeutic and/or preventive strategies of osteosarcoma [13, 19]. One of the earliest models is a spontaneous osteosarcoma model in canines [20–22]. However, this model can be inefficient, expensive, and can take years to develop spontaneous tumors. Conversely, mouse models are less expensive and experiments can be carried out in a reasonable amount of time. Syngeneic mouse models use mouse osteosarcoma cell lines that developed spontaneously [23]. One disadvantage is that the cells are derived from an osteosarcoma that developed in a mouse and therefore is not human tissue. There are also xenograft models used by many investigators. However, the cell lines used are transformed cells lines [19, 24, 25]. Two common agents for transformation are the oncogene ki-ras (as in the 143B line) and the mutagen *N*-methyl-*N*′-nitro-*N*-nitrosoguanidine (MNNG) (as in the HOS/MNNG line) [26, 27]. A disadvantage of using a transforming agent is that it may alter the original genetic events that existed in the osteosarcoma cells when derived from patients.

We sought to establish an osteosarcoma cell line that is highly metastatic but have not been transformed via additional exogenous means. By employing the commonly used and marginally metastatic MG63 human osteosarcoma cell line, we have established such a highly metastatic subline. The parental MG63 cell line was first established 30 years ago from a 14-year-old male with osteosarcoma [28]. We have serially passaged this cell line in athymic nude mice and established a subline (MG63.2), which is highly metastatic compared to the parental line. The two lines were characterized in vitro for cell proliferation, adhesion, migration, and invasion. The two lines were also examined in vivo for tumor formation, as well as for the development of spontaneous pulmonary metastasis from orthotopic implantation of tumor cells. Furthermore, both lines were examined for their expression of genes that have been linked with altered metastatic potential such as matrix metalloproteinases (MMPs), tissue inhibitors of metalloproteinases (TIMPs), and ezrin. Our results demonstrate that the MG63.2 cells exhibit decreased cell adhesion, increased migration and invasion, and increased spontaneous pulmonary metastases in vivo. Furthermore, we have found that the MG63.2 cells have decreased expression of MMPs and increased expression of TIMPs as well as increased expression of ezrin. Thus, this newly established line should be a valuable resource to further the basic and translational research efforts on human osteosarcoma.

## Materials and methods

### Tissue culture and chemicals

The MG63 human osteosarcoma line was purchased from ATCC (Manassas, VA), and maintained in complete DMEM containing 10% fetal bovine serum (FBS, HyClone, Logan, UT), 100 units of penicillin, and 100 μg of streptomycin. MG63 cells were transfected with pEGFP-C1 (Clontech, Palo Alto, CA) with LipofectAMINE (Invitrogen, Carlsbad, CA) according to the manufacture's protocol. At 48 h after transfection, the top 1–2% of transfected cells expressing GFP was sorted by FACS (Fluorescence Activated Cell Sorting) and plated onto 96-well plates. The sorted cells were selected in G418 (0.3 mg/ml) and the clones were expanded. GFP positive clones (>20 clones) were pooled. The pooled cells were transduced using a retroviral vector expressing firefly luciferase and a blasticidin selection marker. Luciferase activity of the pooled stable cells was assessed using the Promega Luciferase Assay system (Promega, Madison, WI). Cells tagged with green fluorescence protein (GFP) and luciferase were maintained in 0.3 mg/ml of G418 and 4 μg/ml of blasticidin S (Invitrogen). Unless otherwise indicated, all chemicals were purchased from Sigma–Aldrich (St. Louis, MO) or Fisher (Pittsburgh, PA).

### Total RNA isolation and RT-PCR analysis

Subconfluent cells were seeded in culture flasks in culture medium supplemented with 1% fetal calf serum. After the indicated treatments, total RNA was isolated using TRIZOL Reagents (Invitrogen) according to the manufacturer's instructions. RT-PCR analysis was carried out as previously described [29]. Briefly, 10 μg of total RNA were used to generate cDNA templates by reverse transcription with hexamer and Superscript II reverse transcriptase (Invitrogen). The RT-PCR primers were designed by using the Primer3 program (http://frodo.wi.mit.edu/cgi-bin/primer3/primer3_www.cgi). The primer sequences are as follows: MMP-2, 5′-cttccgtctgtcccaggat-3′ and

5′-ctgagcgatgccatcaaat-3′; MMP-9, 5′-cccggaccaaggatacagt-3′ and 5′-gccattcacgtcgtcctta-3′; TIMP-1, 5′-ggggcttcaccaagaccta-3′ and 5′-aaggtgacgggactggaag-3′; TIMP-2, 5′-aggaatcggtgaggtcctg-3′ and 5′-acacaagcccggataaagc-3′; and Ezrin, 5′-gctgtgcaggccaagttt-3′ and 5′-tcccactggtccctggta-3′. All samples were normalized with GAPDH. Duplicate reactions were performed in at least three independent batches.

### Western blot analysis

Western blot analysis was performed as previously reported [30]. The cells were collected and lysed in Laemmli sample buffer (non-reducing condition for MMP-9). Cleared total cell lysate was denatured by boiling and loaded onto an 8% SDS–polyacrylamide gel ($\sim$10 μg total proteins per lane). After electrophoretic separation, proteins were transferred to an Immobilon-P membrane (Millipore, Bedford, MA) via electroblotting. The membrane was blocked with 5% nonfat milk in TBST (10 mM Tris–HCl, pH 8.0, 150 mM NaCl, 0.05% Tween-20) at room temperature for 1 h and probed with an anti-MMP-2 (EMD Chemicals, San Diego, CA), anti-MMP-9 (EMD Chemicals, San Diego, CA), anti-TIMP-1 (Triple Point Biologics, Forest Grove, OR), anti-TIMP-2 (EMD Chemicals, San Diego, CA), anti-ezrin, or anti-$\beta$-actin antibodies for 60 min, followed by a 30-min incubation with a secondary anti-mouse or anti-rabbit antibody conjugated with horseradish peroxidase (Pierce, Rockford, IL). All antibodies are from Santa Cruz Biotechnology, Santa Cruz, CA unless otherwise indicated. The presence of the respective protein was detected by using the SuperSignal West Pico Chemiluminescent Substrate kit (Pierce Biotechnology, Rockford, IL) and recorded using the Kodak 440CF ImageStation (Kodak, Rochester, NY).

### Cell adhesion assay

The cell adhesion assay was performed as previously reported [19, 31]. Briefly, 96-well plates were coated with 10 μg/ml of rat tail type I collagen (BD Biosciences, Bedford, MA). The wells were blocked with 1% BSA and $1 \times 10^4$ cells in 0.1% BSA were added to the wells in triplicate. At 15 and 30 min, the wells were washed to remove unattached cells and fixed in formalin. The cells were stained with 1% methylene blue in 0.01 M borate buffer pH 8.5 and washed. The methylene blue was extracted with ethanol and 0.1 M HCl and absorbance was read at 630 nm using a microplate photometer. A standard curve was created with known number of cells per well. The assay was repeated in at least three batches. Statistical analysis was performed using a two-tailed Student's *t*-test.

### Cell migration assay

The cell migration assay was performed using a Boyden chamber migration assay as previously reported [19]. Briefly, exponentially growing cells were trypsinized and washed in DMEM/0.1% BSA medium twice. Pre-equilibrated media containing FBS as a chemoattractant was placed into the bottom chamber of a 6-well transwell unit (Corning Costar, Corning, NY). About $5 \times 10^4$ cells were placed onto each upper chamber of the transwell unit, in which the polycarbonate 8 μm pore membrane was pre-coated with 100 μg/ml of rat tail type I collagen (BD Biosciences) overnight and washed in PBS. The cells were allowed to migrate at 37°C and 5% $CO_2$ for 3 h. The unattached cells were rinsed off with PBS and the membranes containing attached cells were fixed in 10% formalin and washed with PBS. The cells were stained with hematoxylin and rinsed with water. Cells on the unmigrated side were gently wiped off with a wet cotton tip applicator and the membrane was rinsed with water. The membranes containing the migrated cells were dried, and mounted onto slides with Permount. The number of migrated cells per high power field (hpf) was determined by averaging 20 randomly counted hpfs. The assays were performed in triplicate and were reproducible in at least three batches of independent experiments. Statistical analysis was performed using a two-tailed Student's *t*-test.

### Cell invasion (Matrigel) assay

The Matrigel cell invasion assay was performed as previously described [30, 32]. Briefly, polycarbonate membranes with 8 μm pores were coated with 0.5 mg/ml Matrigel (BD Biosciences) overnight. The membranes were rehydrated and $1 \times 10^5$ cells were placed onto each upper chamber of the transwell unit. Media with 10% FBS was used as a chemoattractant in the bottom chamber. The cells were allowed to invade at 37°C and 5% $CO_2$ for 24 h. Cells were fixed in 10% formalin and washed with PBS. The cells were stained with hematoxylin and rinsed with water. Cells on the unmigrated side were gently wiped off with a wet cotton tip applicator and the membrane was rinsed with water. The membranes containing the migrated cells were dried, and mounted onto slides with Permount. The number of migrated cells per hpf was determined by averaging 20 randomly counted hpfs. The assays were performed in triplicate and were reproducible in at least three batches of independent experiments. Statistical analysis was performed using a two-tailed Student's *t*-test.

### Cell proliferation assay

Exponentially growing cells were plated onto 6-well plates ($7.5 \times 10^4$ per well). On each subsequent day, the cells from wells for each cell line were harvested by trypsinization. The number of viable cells, as determined by trypan blue staining, was counted at indicated time points in triplicate. Doubling time was calculated as follows: $t = h \times \ln(2)/\ln(c2/c1)$ in the log phase of growth. Statistical analysis was performed using a two-tailed Student's *t*-test.

### Animal injections

The orthotopic tumor cell injection was performed as previously described [19]. Four- to six-week-old male athymic nude (*nu/nu*) mice were purchased from Harlan Sprague Dawley (Indianapolis, IN). Animal care and use followed the approved IACUC guidelines. For the intratibial injections, exponentially growing osteosarcoma cells were harvested, counted, and resuspended in PBS. About $2 \times 10^6$ cells in 50 µl of PBS were injected into the right proximal tibia. Briefly, the animals were anesthetized with ketamine (80 mg/kg) and xylazine (7 mg/kg). The knee of the nude mouse was flexed beyond 90° and a 50 µl of the cell suspension was injected into the proximal tibia using a 27 gauge needle.

### In vivo selection process

For the selection process to establish the highly metastatic subline, the mice were euthanized at 8–10 weeks. Metastatic nodules were dissected from normal lung tissue using bright field and fluorescent dissection microscopy. The harvested tissue was minced and treated with collagenase (10 mg/ml) for 30 min in an orbital shaker at 37°C. The cells were plated and cultured in the presence of G418. Cells were expanded and repassaged in the animals for additional rounds.

### Xenogen whole body bioluminescence imaging

Animals were anesthetized with isofluorane via a nose-cone mask within the Xenogen IVIS 200 imaging system. The animals were injected (i.p.) with D-luciferin sodium salt (Gold BioTechnology) at 100 mg/kg in 0.1 ml sterile saline. The pseudoimages were obtained by superimposing the emitted light over the gray-scale photographs of the animals. Quantitative analysis as representation of primary tumor volumes was done with the Xenogen's Live Imaging V2.50.1 software. Images were obtained weekly and average signals in photons/second/cm$^2$/steradian were calculated. Comparisons on the weekly signals were performed using a two-tailed Student's *t*-test.

### Histologic evaluations

The animals were euthanized in a carbon dioxide chamber. The primary tumors and the lungs were harvested at necropsy and fixed in Cal-Ex decalcifying solution or 10% formalin overnight, respectively. The fixed samples were then embedded in paraffin and three non-sequential serial sections through the largest coronal portion of the lung per animal were obtained. The sections were stained with hematoxylin and eosin, and analyzed for metastases by microscopy. The total number of metastases per lung section was counted at 100× magnification and averaged among the animals. Three lung sections per animal were counted and averaged. A metastasis was defined as a cluster of greater than five cells and not contiguous with any other metastasis seen at 100× magnification. To quantify the number of pulmonary metastases in the parental MG63 and highly metastatic MG63.2 cells, five animals per time point were euthanized at 6, 8, and 10 weeks for the MG63 group and 6 and 8 weeks for the MG63.2 groups. Animals in the MG63.2 group were not included in the 10 week time point because many of these animals succumbed to their metastatic disease by 8–9 weeks. Histologic counting of the number of metastases was restricted to the 6 week time point because some of the MG63.2 animals died from their metastatic disease at the 8 week time point. This ensured equal number of animals in each group. Statistical analysis was performed using a two-tailed Student's *t*-test.

## Results

### Establishment of the highly metastatic MG63.2 cells

We screened a number of human osteosarcoma cell lines (MG63, TE85, MNNG/HOS, 143B, U20S, and SaOS-2) to identify lines that are tumorigenic in athymic nude mice when implanted into the tibia [19]. Among these lines we identified the MG63 cell line to be tumorigenic but not exogenously transformed. The MG63 cell line was then tagged with GFP via lipofectamine transfection. The stable clones were sorted by FACS. The pooled populations of stable clones were then tagged with firefly luciferase by retroviral transduction and pooled stable clones sorted. As shown in Fig. 1a, the cells were injected into proximal tibiae of nude mice and the occasional pulmonary metastases that developed were harvested using a fluorescent dissection microscope (Fig. 1b). The cells were selected by their drug resistance, expanded, and re-passaged through the animals. The highly metastatic MG63.2 cell line was

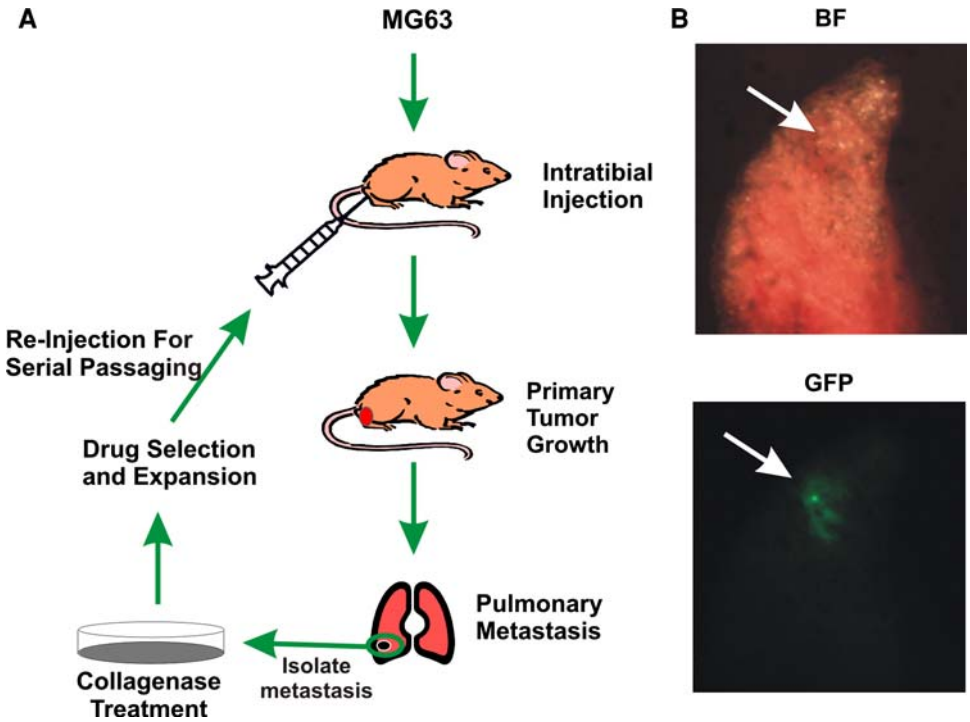


**Fig. 1** Establishment of the highly metastatic subline. **a** A diagram of the selection process for the establishment of the highly metastatic MG63.2 subline is shown. The parental MG63 cells tagged with GFP were injected into the proximal tibiae of nude mice. The lungs were harvested at 8–10 weeks and pulmonary nodules dissected out, treated with collagenase, expanded, and re-injected into animals. **b** A representative metastatic nodule (*arrow*) that is visible under fluorescent (GFP) but not bright field (BF) microscopy. The GFP tag allowed for harvesting of the metastatic nodule and repassaging through the animals

established after of two rounds of passaging through the animals.

## The highly metastatic MG63.2 cells exhibited a slightly slower proliferation rate compared to the parental MG63 cells

We next sought to characterize the MG63.2 cells for in vitro phenotypes important for tumorigenesis and metastasis. We first examined MG63 and MG63.2 cells for their in vitro proliferation. Qualitatively, we noticed that the MG63.2 cells tended to grow at a slightly slower rate than the parental. Cells were plated in triplicate and on subsequent days, the cells were trypsinized as counted. As shown in Fig. 2a, the highly metastatic MG63.2 cells exhibited a lower in vitro proliferation rate than that of the parental ($P$ value $< 0.023$). The average doubling time for the parental MG63 cells is 28.3 h compared to 36.1 h for the highly metastatic MG63.2 cells.

## The highly metastatic MG63.2 cells exhibited decreased cell adhesion and increased cell migration and invasiveness

Cell migration, invasion, and adhesion are essential phenotypes for cancer metastasis [33–36]. In order for a cell to migrate and metastasize, it first must overcome local adhesive forces [33, 34]. We first examined the two cell lines for their ability to adhere to Type I collagen, the most predominant matrix protein in bone. As shown in Fig. 2b, the highly metastatic MG63.2 cells had decreased relative adherence compared to the parental MG63 cells. At the 15 and 30 min time points, the decrease in relative adherence ranged from 25 to 32% ($P$ value $< 0.02$).

Cell migration is also an important indicator of metastatic potential. We next examined the parental MG63 and highly metastatic MG63.2 cells for their ability to migrate in a Boyden chamber migration assay. The cells were plated onto the polycarbonate membrane containing 8 μM pores and coated with Type I collagen. Type I collagen was chosen because it is the most predominant extracellular protein in bone. As shown in Fig. 3a, b, the MG63.2 cells had a greater migratory capacity compared to the parental. Specifically, there was a 53% increase in migration in the MG63.2 cells ($P$ value $< 0.0003$).

Since invasion is one of the critical early steps in metastasis, we next examined the MG63 parental and MG63.2 cells for invasiveness. As we have described previously [30], the membranes were coated with Matrigel (BD Biosciences, Bedford, MA) and the cells are allowed to invade across. As shown in Fig. 3c, d, the MG63.2 cells have a greater ability to invade through the matrix compared to the parental MG63 cells. There was a greater than fourfold increase in the number of cells that invaded across ($P$ value $< 0.000032$).

## The highly metastatic MG63.2 cells developed orthotopic tumors and lung metastases with high efficiency in an animal model

To further characterize the tumorigenic and metastatic phenotypes, we next determined the ability of the MG63

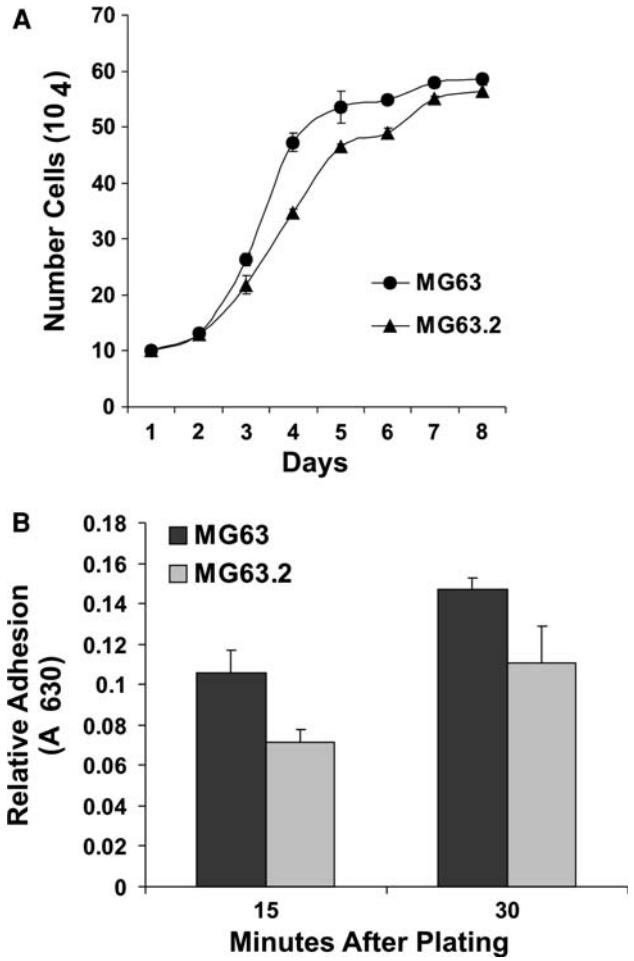


**Fig. 2** In vitro proliferation and cell adhesion. **a** The in vitro growth of the MG63 and MG63.2 cell lines were determined. Cells were plated onto 6-well plates in triplicate. On each subsequent day, the number of viable cells from wells for each cell line was counted. **b** The ability of the MG63 and MG63.2 cells to adhere to a type I collagen matrix, the most predominant matrix protein in bone, was determined. Cells were plated onto a type I collagen matrix and non-adherent cells washed off at the indicated times. The cells were formalin fixed and stained with methylene blue. The methylene blue was extracted and absorbance was read at 630 nm to reflect the relative adhesion. The experiments were performed in triplicate

and MG63.2 cells to form orthotopic tumors and produce spontaneous pulmonary metastases. We have recently used a reliable orthotopic xenograft mouse model to evaluate the potential for human osteosarcoma cell lines to form primary tumors and develop metastases [19]. Here, the MG63 and MG63.2 cells were injected into the proximal tibia of athymic nude mice, animals serially imaged, and the lungs examined at the endpoint. As shown in Fig. 4A, the MG63.2 injected animals developed comparatively larger tumors compared to the parental MG63 cells. The relative tumor burden was determined by quantifying the luciferase activity on the Xenogen whole animal imaging system. As shown in Fig. 4B, the MG63.2 cells formed larger tumors than the parental MG63 cells, which became significant by 3 weeks ($P$ value $< 0.024$). As shown in Fig. 4C for the parental MG63 and Fig. 4D for the MG63.2 cells, the histologic sections of the primary tumors demonstrate malignant cells infiltrating the trabaecular bone with evidence of destruction of the normal bone architecture. The histologic features are similar to osteosarcoma in humans. The images at 20× magnification (Fig. 4C, D) depict the proximal aspect of the tibia with tumor cells within it.

We next compared the metastatic potential of the parental MG63 and the MG63.2 cells. Since the cell lines had been tagged with luciferase, we were able to follow the animals for pulmonary metastases by weekly imaging. As shown in Fig. 5a, pulmonary metastases are easily detectable in the MG63.2 compared to the parental MG63 cells at 4 weeks post-injection. Gross evaluations of the lungs at 6 weeks only demonstrated 0.5–1.0 mm overt metastases that are marginally visible on the surface (data not shown). As shown in Fig. 5b, these small metastases become easily visible by 8 weeks and some animals begin to succumb to their metastatic disease. As exemplified in Fig. 5c, the vast majority of the parental MG63 injected animals did not have any pulmonary metastases. There was an occasional animal that had a few metastases (data not shown). In contrast, animals injected with the MG63.2 cell lines had numerous metastases (Fig. 5c).

To quantify the metastatic potential of the cell lines, animals injected with the respective MG63 or MG63.2 cells were euthanized at 6 weeks and the lungs subjected to histologic evaluation. Non-sequential serial sections through largest coronal portion of the lungs were quantified for the average number of metastases per section. A metastasis was defined as a cluster of at least five cells that was not contiguous with another metastatic lesion at 100× magnification. When number of metastases was counted at the 6 week time point, there was a greater than 200-fold increase in the number of metastases between the parental MG63 and highly metastatic MG63.2 cells, $P$ value $< 0.003$ (Fig. 6a, b). At the 10 week time point, we found that the parental MG63 injected animals continued to have significantly fewer metastases when compared to the highly metastatic MG63.2 injected animals ($P$ value $< 0.004$), which were sacrificed at 6 weeks (Fig. 6b). We were unable to consistently evaluate the MG63.2 injected animals at the later 10 week time point because many of these animals begin to succumb to their metastatic disease by 8 weeks. In separate experiments, we have allowed some of the parental MG63 injected animals to extend to 12 weeks and the number of metastases, again, remain dramatically lower compared to the MG63.2 injected animals at the 6 week time point (data not shown).

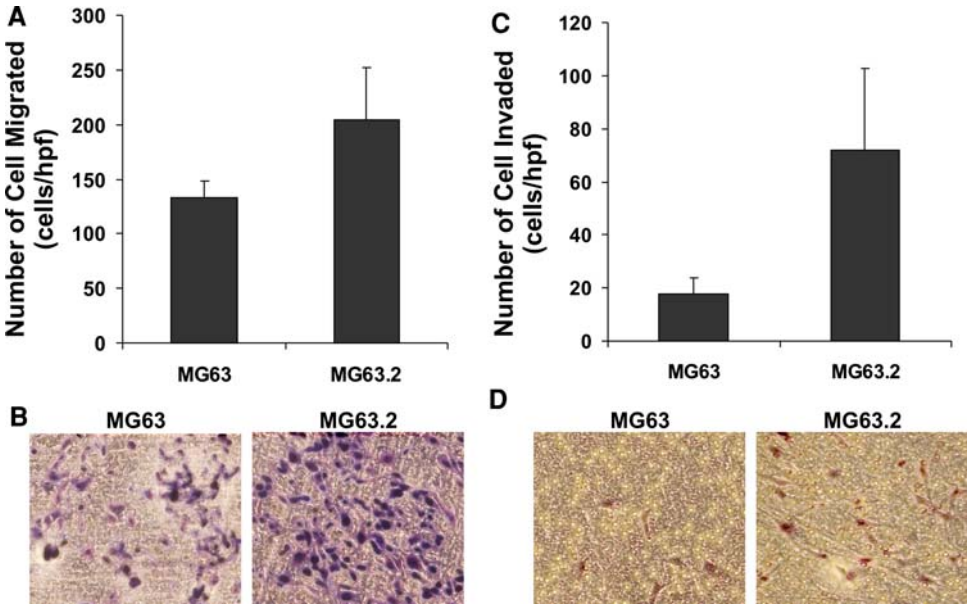


**Fig. 3** Cell migration and cell invasion. **a** Cell migration was assessed by a Boyden chamber migration assay. Cells were plated onto a porous Transwell polycarbonate membrane coated with type I collagen. The cells were allowed to migrate across the membrane using fetal bovine serum as a chemoattractant. The cells were formalin fixed and stained. Cells that have not migrated across were removed and the number of cells that have migrated was counted. **b** Representative sample of a high power field of the migrated cells for two cell lines. **c** Cell invasion was assessed by a Matrigel cell invasion assay. Cells were plated onto a porous Transwell polycarbonate membrane coated with a layer of Matrigel. Fetal bovine serum was used as a chemoattractant. The number of cells that invaded across the membrane was counted. **d** Representative sample of a high power field of the invaded cells for the two cell lines

### Expression of metastasis-associated genes in MG63 and MG63.2 cells

Matrix metalloproteinases, TIMPs, and ezrin are well-recognized genes associated with metastasis [32, 37–40]. We next examined the expression of MMP-2, MMP-9, TIMP-1, TIMP-2, and ezrin in the parental MG63 and highly metastatic MG63.2 cells. Semi-quantitative RT-PCR and Western blot analysis were performed on the two cell lines. As shown in Fig. 7a–c, we found that MMP-2 and MMP-9 expression were decreased in the highly metastatic MG63.2 cells compared to the MG63 cells. TIMP-2 expression was elevated in the metastatic MG63.2 cells. There was no substantial difference in TIMP-1 expression between the lines. Finally, ezrin expression was elevated in the highly metastatic MG63.2 cells compared to that of the parental MG63 cells.

## Discussion

In this report, we established a highly metastatic human osteosarcoma cell line from a parental line that is marginally metastatic. Animals injected with the MG63.2 cells readily form spontaneous pulmonary metastases compared to those injected with the parental MG63 cells. This model is unique in that it uses non-transformed human osteosarcoma cell lines. Other animal models use mouse cell lines or transformed human osteosarcoma cell lines [19, 23, 24, 41]. Specifically, some of these xenograft models employ human osteosarcoma cells that have been transformed with ki-ras or the mutagen MNNG, which can significantly alter gene expression in these lines [26, 27]. The canine spontaneous osteosarcoma model is a valuable tool but has the disadvantage of expense and the time to develop tumors[20–22].

Potentially, the highly metastatic MG63.2 cell line established here can be used as an investigative tool to examine tumor formation and metastasis in mice without concerns about the bystander effect of viral or mutagenic transformation. It is conceivable that gene expression profiling between the highly metastatic MG63.2 and parental MG63 cells may be useful to identify novel genes that modulate metastasis. The newly identified genes can then be examined for their effects on metastasis in the animal model. We are currently embarking such a line of investigation.

As expected, the highly metastatic MG63.2 cells had increased cell migration and invasion while cell adhesion was decreased relative to the parental MG63 cells. Cell migration, invasion, and adhesion are all important phenotypes for early events in the metastatic cascade [35, 36]. Alterations in these phenotypes facilitate osteosarcoma

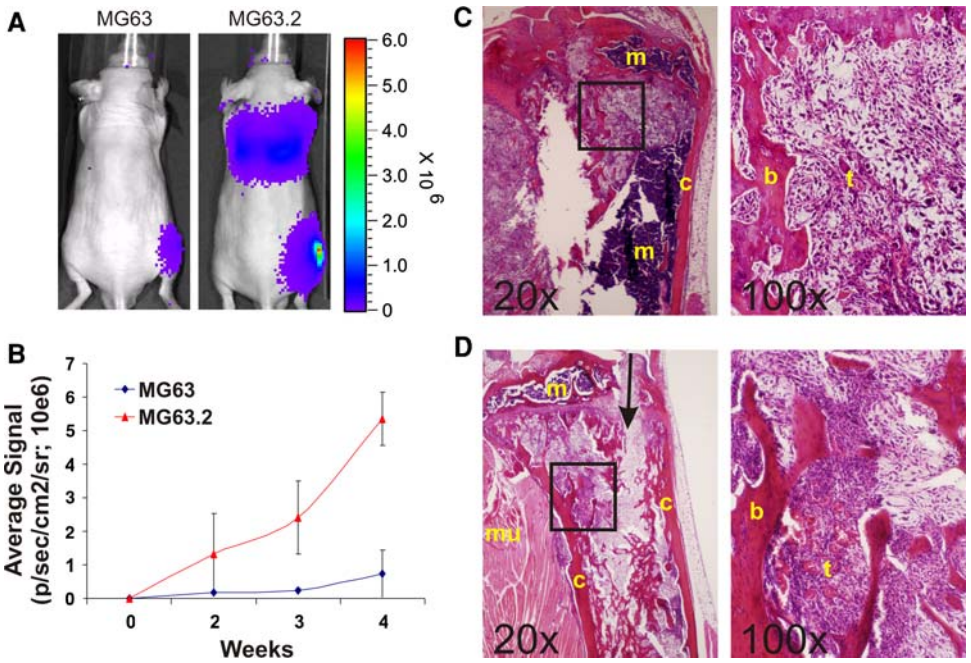


**Fig. 4** Primary tumor growth and histology. **A** MG63 and MG63.2 cells were injected into the proximal tibiae of nude mice. The tumors were allowed to form and weekly Xenogen bioluminescent images were taken. Representative images taken at 4 weeks show that the MG63.2 primary tumors are larger than the parental MG63. **B** The size of the tumor (in photons/sec/cm$^2$/steradian) was calculated by using the Xenogen Living Imaging Software. The MG63.2 injected animals ($n = 5$) formed larger tumors compared to the parental MG63 and became significant by 3 weeks ($P$ value $< 0.024$). Sample histology of the primary tumor site is shown for the MG63 (**C**) and MG63.2 (**D**) cell lines. The proximal tibiae of the animals were sectioned sagitally and stained with hematoxylin and eosin. Images taken at $\times 20$ and $\times 100$ are shown. Tumors grew within the bone and in many cases, expanded beyond the bone cortex. Note that the trabecular bone is often destroyed by the tumor. The needle track for the injections can be seen in some of the sections (*arrow*). Abbreviations: (*m*) marrow, (*mu*) muscle, (*b*) trabecular bone, (*c*) bone cortex, and (*t*) tumor

cells to overcome local adhesive forces, migrate towards the microvasculature, and invade the vessels. Our serial passaging process likely selected for cells with these aggressive phenotypes.

We find that the MG63.2 cells have increased expression of ezrin. Ezrin is a cytoskeletal linkage protein that that has been associated with metastasis. Our finding on increased ezrin expression in the highly metastatic MG63.2 cells is consistent with other reports on the association between ezrin expression and osteosarcoma metastasis [37, 38]. Ezrin expression is up-regulated in high grade osteosarcoma samples and increased expression is correlated with decreased survival [42, 43]. The association of increased ezrin expression and metastasis is also seen in a number of cancers including rhabodomyosarcoma, uveal malignant melanoma, and pancreatic cancer [44]. Interestingly and in contrast, increased expression of ezrin in Ewing's sarcoma is associated with decreased tumor growth and metastasis [45]. Our findings of increased motility and decreased adhesion may be in part related to the increased expression of ezrin. Through its function as a cytoskeletal linker protein and its interactions with CD44, ezrin has been shown to play an important role in cell adhesion, motility, and tumor–endothelium interactions in metastasis [46].

Interestingly, we find that the metastatic MG63.2 cells have decreased expression of MMP-2 and MMP-9. This is in contrast to other reports of increased expression of MMP-2 and MMP-9 associated a number of human cancers including human osteosarcoma [32, 39, 40]. Despite our findings of decreased MMP expression, the metastatic MG63.2 cells demonstrated greater invasion ability in vitro compared to the parental MG63 line. It is likely that the phenotype is independent of the MMPs examined. In correlation with our findings on the MMP expression, we find that the MG63.2 cells have increased expression of TIMP-2. TIMP-1 expression was relatively similar between the two lines. Ferrari et al. demonstrated that serum levels of TIMP-1 were higher in patients who had metastasis at diagnosis as well as those who later developed metastases or local recurrences [39].

We found that the highly metastatic MG63.2 cells grew at a slightly slower rate in vitro compared to the parental, while in vivo tumor growth of the MG63.2 cells was greater than the parental. The in vitro findings are similar the findings by Khanna et al. who established a highly metastatic subline of a mouse osteosarcoma cell line and found that this line grew at a slower rate compared to the parental [23]. In our study, there was a clear difference in

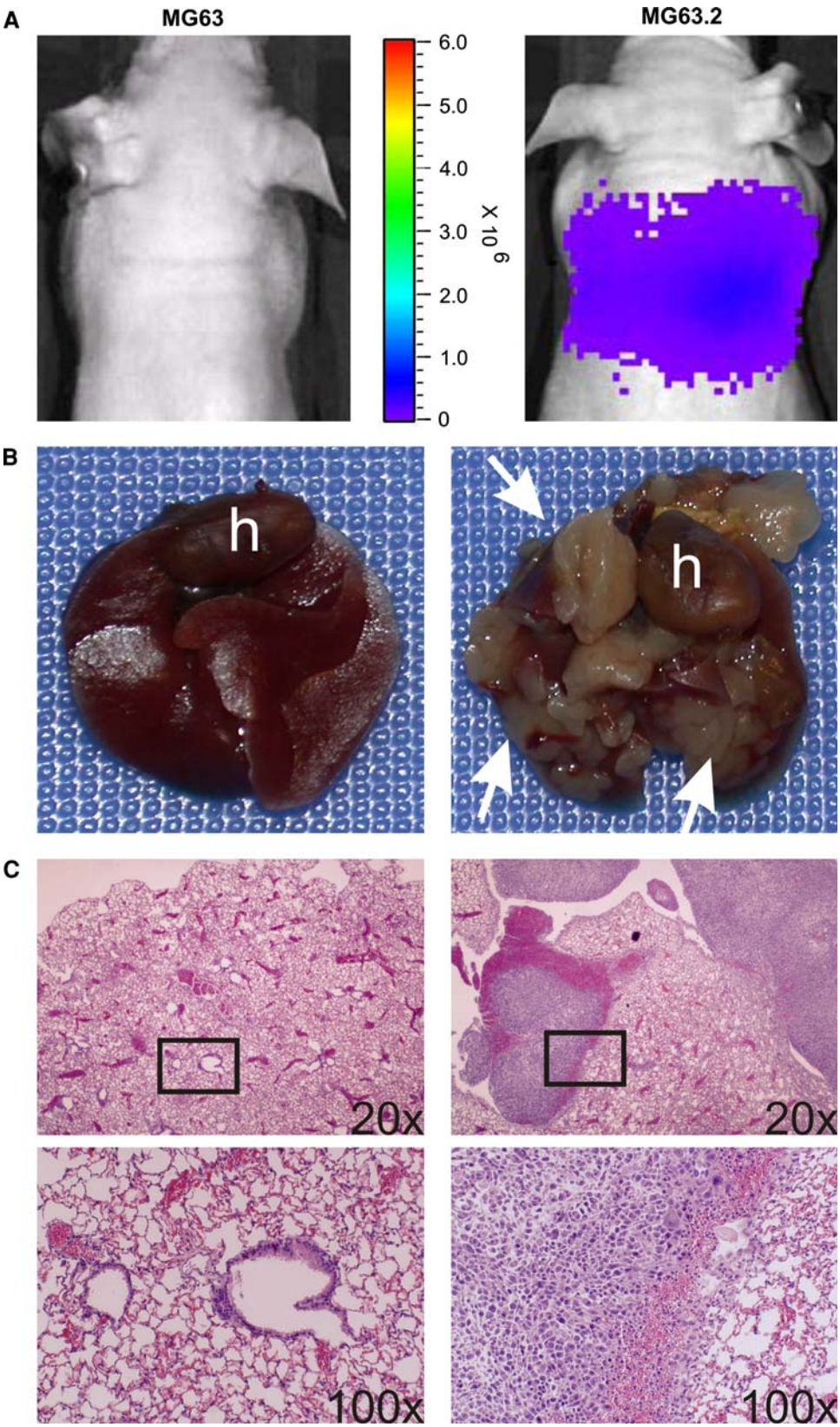


**Fig. 5** Pulmonary metastases. **a** MG63.2 injected animals readily develop pulmonary metastases. A sample Xenogen image taken at 4 weeks post-injection is demonstrating the detectable signal in the lungs. **b** Gross images of lungs harvested from animals at 8 weeks post-injection are shown demonstrating that the pulmonary nodules (*arrows*) are clearly visible on the MG63.2 injected animals. For reference, the heart of the animal is indicated, (*h*). **c** The corresponding hematoxylin and eosin sections of the lungs at ×20 and ×100 are shown

the tumor growth between the two cell lines when injected orthotopically into the proximal tibiae of nude mice. The highly metastatic MG63.2 cells formed larger tumors. The difference in the in vivo tumor formation may reflect the different tumorigenic potential between the lines. Li et al. recently reported on orthotopic implantation of MG63 cells

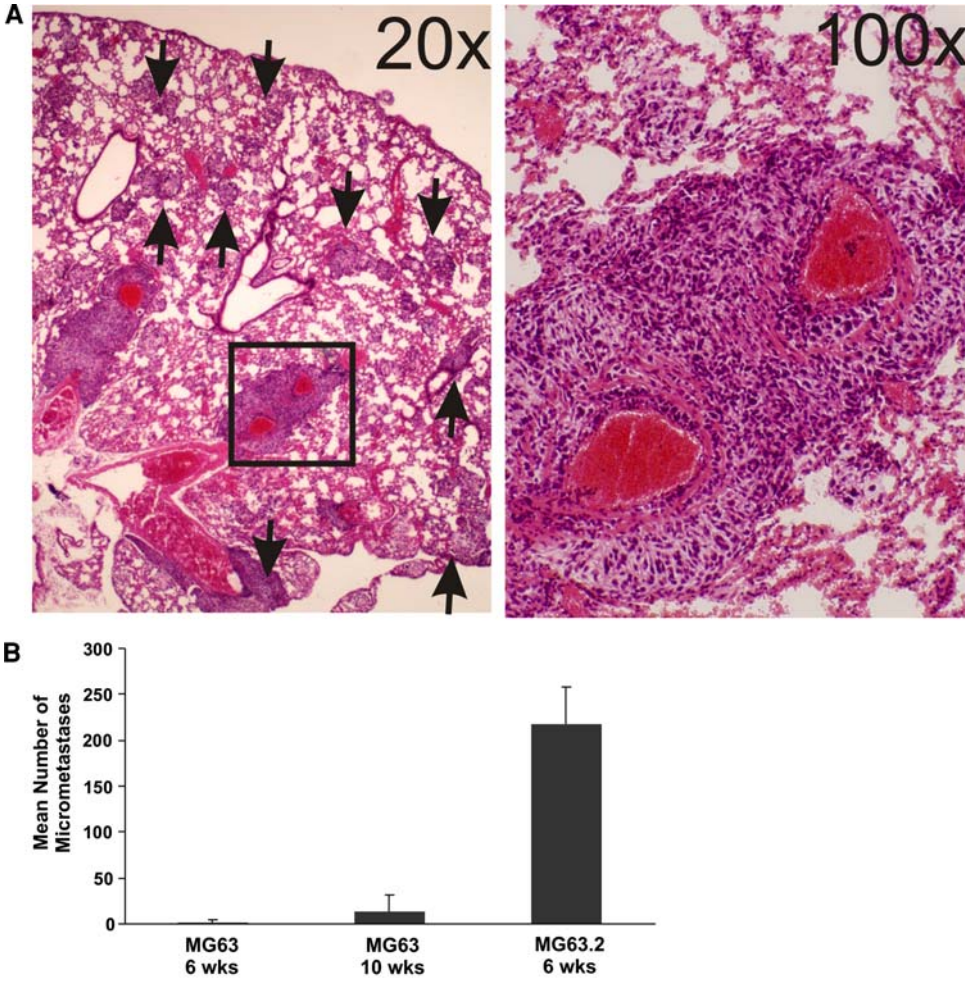


**Fig. 6** Quantification of pulmonary metastases. To quantify the number of metastatic lesions, the animals were sacrificed at the indicated time points. Three non-sequential serial sections through the largest coronal portion of the lungs were obtained and the mean number of micrometastases was counted per lung section. **a** An image of a representative lung section from an MG63.2 injected animal is shown at ×20 and ×100. Some of the micrometastases are indicated by *arrows*. **b** The average number of metastasis was counted at ×100 magnification and depicted for the indicated time points

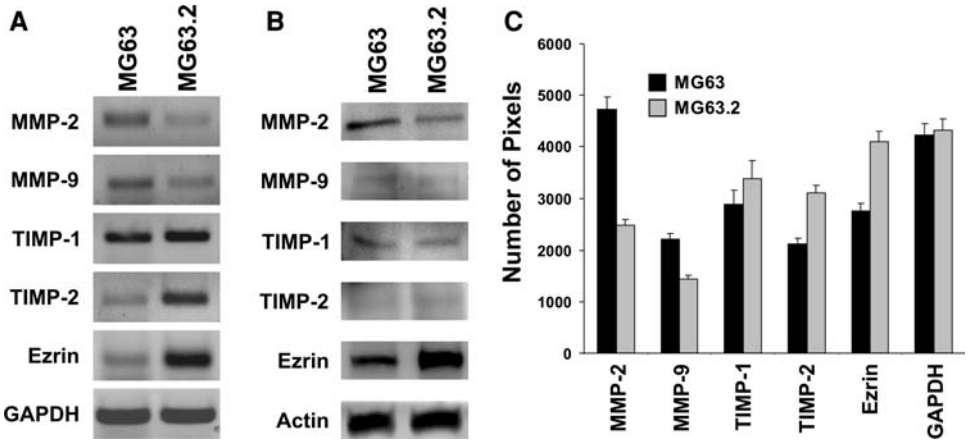


**Fig. 7** Expression of known metastasis-associated genes. **a** Expression of MMP-2, MMP-9, TIMP-1, TIMP-2, and ezrin was determined by semi-quantitative RT-PCR as described in "Materials and methods". **b** Western blot analysis for MMP-2, MMP-9, TIMP-1, TIMP-2, and ezrin was performed. **c** Densitometry scan for the semi-quantitative RT-PCR results was performed and calculated

in nude mice [47]. However, this study focused only on the primary tumor and did not examine metastases.

In summary, we have established a highly metastatic human cell line from a parental line that is marginally metastatic. We believe that this line is unique in that it is a human osteosarcoma cell line that has not been transformed exogenously, and can be used as a valuable tool in dissecting out the basic mechanism in the progression of osteosarcoma as well as a tool in investigating novel therapies.

**Acknowledgments** This work was funded by the Orthopaedic Research and Education Foundation (HHL, TCH and RCH), the Brinson Foundation (HHL, TCH and RCH), the American Cancer Society (HHL and TCH), and the National Institute of Health (HHL, TCH and RCH). We would like to thank Dr. Ernst Lengyel for providing the MMP-2, MMP-9, TIMP-1, and TIMP-2 antibodies.

## References

1. Murphey MD, Robbin MR, McRae GA et al (1997) The many faces of osteosarcoma. Radiographics 17(5):1205–1231
2. Whelan JS (1997) Osteosarcoma. Eur J Cancer 33(10):1611–1618. doi:10.1016/S0959-8049(97)00251-7 (discussion 8–9)
3. Link MP, Goorin AM, Miser AW et al (1986) The effect of adjuvant chemotherapy on relapse-free survival in patients with osteosarcoma of the extremity. N Engl J Med 314(25):1600–1606
4. Ward WG, Mikaelian K, Dorey F et al (1994) Pulmonary metastases of stage IIB extremity osteosarcoma and subsequent pulmonary metastases. J Clin Oncol 12(9):1849–1858
5. Kaste SC, Pratt CB, Cain AM et al (1999) Metastases detected at the time of diagnosis of primary pediatric extremity osteosarcoma at diagnosis: imaging features. Cancer 86(8):1602–1608. doi:10.1002/(SICI)1097-0142(19991015)86:8<1602::AID-CNCR31>3.0.CO;2-R
6. Yonemoto T, Tatezaki S, Ishii T et al (1998) Prognosis of osteosarcoma with pulmonary metastases at initial presentation is not dismal. Clin Orthop Relat Res 349:194–199. doi:10.1097/00003086-199804000-00024
7. Jaffe N, Pearson P, Yasko AW et al (2003) Single and multiple metachronous osteosarcoma tumors after therapy. Cancer 98(11):2457–2466. doi:10.1002/cncr.11800
8. Kim SJ, Choi JA, Lee SH et al (2004) Imaging findings of extrapulmonary metastases of osteosarcoma. Clin Imaging 28(4):291–300. doi:10.1016/S0899-7071(03)00206-7
9. Kager L, Zoubek A, Potschger U et al (2003) Primary metastatic osteosarcoma: presentation and outcome of patients treated on neoadjuvant Cooperative Osteosarcoma Study Group protocols. J Clin Oncol 21(10):2011–2018. doi:10.1200/JCO.2003.08.132
10. Mankin HJ, Hornicek FJ, Rosenberg AE et al (2004) Survival data for 648 patients with osteosarcoma treated at one institution. Clin Orthop Relat Res 429:286–291. doi:10.1097/01.blo.0000145991.65770.e6
11. Stiller CA, Craft AW, Corazziari I (2001) Survival of children with bone sarcoma in Europe since 1978: results from the EUROCARE study. Eur J Cancer 37(6):760–766. doi:10.1016/S0959-8049(01)00004-1
12. Solheim OP, Saeter G, Elomaa I et al (1992) The treatment of osteosarcoma: present trends. The Scandinavian Sarcoma Group experience. Ann Oncol 3(Suppl 2):S7–S11
13. Tang N, Song WX, Luo J et al (2008) Osteosarcoma development and stem cell differentiation. Clin Orthop Relat Res 466(9):2114–2130. doi:10.1007/s11999-008-0335-z
14. Gorlick R, Anderson P, Andrulis I et al (2003) Biology of childhood osteogenic sarcoma and potential targets for therapeutic development: meeting summary. Clin Cancer Res 9(15):5442–5453
15. Sandberg AA, Bridge JA (2003) Updates on the cytogenetics and molecular genetics of bone and soft tissue tumors: osteosarcoma and related tumors. Cancer Genet Cytogenet 145(1):1–30. doi:10.1016/S0165-4608(03)00105-5
16. Pakos EE, Kyzas PA, Ioannidis JP (2004) Prognostic significance of TP53 tumor suppressor gene expression and mutations in human osteosarcoma: a meta-analysis. Clin Cancer Res 10(18 Pt 1):6208–6214. doi:10.1158/1078-0432.CCR-04-0246
17. Feugeas O, Guriec N, Babin-Boilletot A et al (1996) Loss of heterozygosity of the RB gene is a poor prognostic factor in patients with osteosarcoma. J Clin Oncol 14(2):467–472
18. Yokoyama R, Schneider-Stock R, Radig K et al (1998) Clinicopathologic implications of MDM2, p53 and K-ras gene alterations in osteosarcomas: MDM2 amplification and p53 mutations found in progressive tumors. *Pathology*. Res Pract 194(9):615–621
19. Luu HH, Kang Q, Park JK et al (2005) An orthotopic model of human osteosarcoma growth and spontaneous pulmonary metastasis. Clin Exp Metastasis 22(4):319–329. doi:10.1007/s10585-005-0365-9
20. Misdorp W, Hart AA (1979) Some prognostic and epidemiologic factors in canine osteosarcoma. J Natl Cancer Inst 62(3):537–545
21. Hahn KA, Legendre AM, Schuller HM (1997) Amputation and dexniguldipine as treatment for canine appendicular osteosarcoma. J Cancer Res Clin Oncol 123(1):34–38. doi:10.1007/BF01212612
22. Haines DM, Bruland OS, Matte G et al (1992) Immunoscintigraphic detection of primary and metastatic spontaneous canine osteosarcoma with F(ab')2 fragments of osteosarcoma-associated monoclonal antibody TP-1. Anticancer Res 12(6B):2151–2157
23. Khanna C, Prehn J, Yeung C et al (2000) An orthotopic model of murine osteosarcoma with clonally related variants differing in pulmonary metastatic potential. Clin Exp Metastasis 18(3):261–271. doi:10.1023/A:1006767007547
24. Berlin O, Samid D, Donthineni-Rao R et al (1993) Development of a novel spontaneous metastasis model of human osteosarcoma transplanted orthotopically into bone of athymic mice. Cancer Res 53(20):4890–4895
25. McGary EC, Heimberger A, Mills L et al (2003) A fully human antimelanoma cellular adhesion molecule/MUC18 antibody inhibits spontaneous pulmonary metastasis of osteosarcoma cells in vivo. Clin Cancer Res 9(17):6560–6566
26. Rhim JS, Putman DL, Arnstein P et al (1977) Characterization of human cells transformed in vitro by *N*-methyl-*N*′-nitro-*N*-nitrosoguanidine. Int J Cancer 19(4):505–510. doi:10.1002/ijc.2910190411
27. Hensler PJ, Annab LA, Barrett JC et al (1994) A gene involved in control of human cellular senescence on human chromosome 1q. Mol Cell Biol 14(4):2291–2297
28. Heremans H, Billiau A, Cassiman JJ et al (1978) In vitro cultivation of human tumor tissues. II. Morphological and virological characterization of three cell lines. Oncology 35(6):246–252
29. Haydon RC, Zhou L, Feng T et al (2002) Nuclear receptor agonists as potential differentiation therapy agents for human osteosarcoma. Clin Cancer Res 8(5):1288–1294
30. Luo X, Sharff KA, Chen J et al (2008) S100A6 expression and function in human osteosarcoma. Clin Orthop Relat Res 466(9):2060–2070. doi:10.1007/s11999-008-0361-x
31. Oliver MH, Harrison NK, Bishop JE et al (1989) A rapid and convenient assay for counting cells cultured in microwell plates: application for assessment of growth factors. J Cell Sci 92(Pt 3):513–518
32. Radjabi AR, Sawada K, Jagadeeswaran S et al (2008) Thrombin induces tumor invasion through the induction and association of matrix metalloproteinase-9 and beta1-integrin on the cell surface. J Biol Chem 283(5):2822–2834. doi:10.1074/jbc.M704855200
33. Yoshida BA, Sokoloff MM, Welch DR et al (2000) Metastasis-suppressor genes: a review and perspective on an emerging field. J Natl Cancer Inst 92(21):1717–1730. doi:10.1093/jnci/92.21.1717
34. Steeg PS (2005) Cancer biology: emissaries set up new sites. Nature 438(7069):750–751. doi:10.1038/438750b
35. Hajra KM, Fearon ER (2002) Cadherin and catenin alterations in human cancer. Genes Chromosom Cancer 34(3):255–268. doi:10.1002/gcc.10083

36. Skubitz AP (2002) Adhesion molecules. Cancer Treat Res 107:305–329
37. Ogino W, Takeshima Y, Mori T et al (2007) High level of ezrin mRNA expression in an osteosarcoma biopsy sample with lung metastasis. J Pediatr Hematol Oncol 29(7):435–439. doi: 10.1097/MPH.0b013e3180640d18
38. Khanna C, Wan X, Bose S et al (2004) The membrane-cytoskeleton linker ezrin is necessary for osteosarcoma metastasis. Nat Med 10(2):182–186. doi:10.1038/nm982
39. Ferrari C, Benassi S, Ponticelli F et al (2004) Role of MMP-9 and its tissue inhibitor TIMP-1 in human osteosarcoma: findings in 42 patients followed for 1–16 years. Acta Orthop Scand 75(4): 487–491
40. Cho HJ, Lee TS, Park JB et al (2007) Disulfiram suppresses invasive ability of osteosarcoma cells via the inhibition of MMP-2 and MMP-9 expression. J Biochem Mol Biol 40(6):1069–1076
41. Khanna C, Khan J, Nguyen P et al (2001) Metastasis-associated differences in gene expression in a murine model of osteosarcoma. Cancer Res 61(9):3750–3759
42. Park HR, Jung WW, Bacchini P et al (2006) Ezrin in osteosarcoma: comparison between conventional high-grade and central low-grade osteosarcoma. Pathol Res Pract 202(7):509–515. doi: 10.1016/j.prp.2006.01.015
43. Kim MS, Song WS, Cho WH et al (2007) Ezrin expression predicts survival in stage IIB osteosarcomas. Clin Orthop Relat Res 459:229–236. doi:10.1097/BLO.0b013e3180413dbf
44. Hunter KW (2004) Ezrin, a key component in tumor metastasis. Trends Mol Med 10(5):201–204. doi:10.1016/j.molmed.2004.03.001
45. Krishnan K, Bruce B, Hewitt S et al (2006) Ezrin mediates growth and survival in Ewing's sarcoma through the AKT/mTOR, but not the MAPK, signaling pathway. Clin Exp Metastasis 23(3–4):227–236. doi:10.1007/s10585-006-9033-y
46. Martin TA, Harrison G, Mansel RE et al (2003) The role of the CD44/ezrin complex in cancer metastasis. Crit Rev Oncol Hematol 46(2):165–186. doi:10.1016/S1040-8428(02)00172-5
47. Li W, Zeng JC, Pei FX et al (2007) Establishment of orthotopic model of MG-63 osteosarcoma. Sichuan Da Xue Xue BaoYi Xue Ban 38(2):321–323